Fabrication of Narrow-Slit Masks for the Gemini Multi-Object Spectrograph

Kei Szeto, James Stilburn, Tim Bond, Scott Roberts, Jerry Sebesta, Les Saddlemyer

Dominion Astrophysical Observatory,
Herzberg Institute of Astrophysics,
National Research Council Canada
5071 West Saanich Road,
Victoria, British Columbia,
Canada, V8X 4M6

Abstract

The fabrication requirements of the Gemini Multi-Object Spectrograph (GMOS) slit mask is discussed particularly in terms of the slit-to-slit position, slit geometry and the telescope operation. The demand for precision slit masks with high quality slits of width of less than quarter arcsecond and an allowable fabrication time of two hours required examination of innovative fabrication processes and mask materials.

Different fabrication processes including high precision cutting processes, water-jet and laser machininig systems are evaluated according to cost, speed and efficiency, and the findings are documented. Different candidate mask materials including low thermal expansion metals and novel materials such as graphite paper and carbon-fibre composite sheet, are evaluated according to their relevant mechanical and physical properties, and the findings are also documented.

In addition to identifying that the most suitable mask material is unidirectional cabron fibre sheet and the corresponding fabrication process is a Nd:YAG laser machining system, the mask handling system for GMOS is described and methodology to minimize systematic fabrication errors is also proposed.

Keyword: multi-object spectrograph, mask making, slit mask, narrow slit, carbon fibre, laser machining

1. Introduction

GMOS has been specified as the general-purpose optical instrument for both Gemini telescopes in Mauna Kea, Hawaii and Cerro Pachon, Chile. GMOS will offer the following functions:

- Long-slit spectroscopy
- Multi-slit spectroscopy
- Integral-field spectroscopy
- Wide-filed optical imaging

For multi-slit spectroscopy, GMOS imaging capability will be used to provide data suitable for spectroscopic mask production and, in order to exploit the inherently superb image quality of the Gemini telescopes, slit width much narrower than traditionally used will be employed. In addition, the slit opening is required to be of uniform width and free of jagged edges, and each slit must be positioned accurately. These considerations were set by the project scientists in order to satisfy the targeted specifications for spectral resolution, velocity accuracy and sky subtraction.

2. The Requirements

The fabrication of narrow-slit mask requirements are stated in the GMOS Functional Requirements[1] and they can be divided into three categories in terms of the slit geometry, mask material and fabrication.

2.1 Slit Geometry Requirements

- Rectangular Slit
  - width - 0.2 to 5 arcsec., 0.12 mm to 3.1 mm
  - length - 1.6 to 5.5 arcsec.,1 mm to 205 mm
- Curved Slit
  - arbitrary geometry
- Edge Smoothness
  - less than 1% of the narrowest slit width, i.e. 1.2 µm rms
- Edge Parallelism
  - less than 1% variation of width
- End Geometry
  - square or round
- Other Apertures
  - 1.9 mm to 6.3 mm round or square aperture

2.2 Mask Material Requirements

- Maximum Thickness
  - 1 mm
- Maximum Sag Under Gravity Once Mounted
  - the entire mask must remain flat to within 1 mm for any gravity orientation
- Physical Properties
  - opaque from λ = 300 nm to 2,500 nm
  - reflectance at normal incidence not exceeding 10% over the same wavelength range
  - dimensionally stable
  - corrosion resistance
  - blackenable
  - low CTE to meet the slit-to-slit position tolerance w.r.t. the variation in the operating temperature, a range of >10°C is expected

2.3 Mask Fabrication Requirements

- Number of Slits
  - 200 nominal, 600 maximum (3 banks of 200 slits each)
- Size of Mask
  - 206 mm x 206 mm planar mask with round corners of 130.5 mm radius
  - Slit-to-Slit Position Tolerance
    - 5 µm rms, perpendicular to slit direction, i.e. dispersion direction
    - 150 µm rms, parallel to slit direction
- Average Fabrication Time
  - <2 hours for a 200 slit mask

3. Selection of Mask Making System

In order to develop a narrow-slit mask making system, the optimal mask material and slit-cutting process must be identified. Therefore, different materials and precision cutting processes were examined with respect to the GMOS requirements. They were:

- Conventional Metals
  - aluminum, stainless steel
- Low CTE Materials
  - niobium, zirconium, molybdenum, Invar, graphite paper, carbon fibre composite sheet
- High Precision Cutting Processes
  - photo-chemical etching, water-jet cutting, electric discharge machining, computer numerical control machining, laser cutting

3.1 Investigation of Mask Material

Aluminum has been a common mask material with multi-object spectrograpsh such as MOS/SIS at the Canada-France-Hawaii telescope (CFHT), and LRIS and DEIMOS at the Keck telescope. However, aluminum also has a high coefficient of thermal expansion (CTE). Due to the possible temperature variation during operation and its influence on the slit-to-slit position, only materials with CTE lower than stainless steel and are commercially available in thickness of less than 1 mm were considered. The mechanical stiffness of the mask material was another consideration, it should support its own weight such that the maximum sag would not exceed 1 mm. Calculations using simple plate theory showed that the required thickness is at least 0.8 mm for an aluminum plate suspended over a 206 mm square mask opening, assuming that the edges were simply supported. Although by tensioning the mask material the required thickness will decrease, its impact on slit geometry and positions is uncertain.

The mask materials examined are summarised in Table 1. In terms of CTE, the only metal meeting the temperature variation requirements is Invar; and in terms of mechanical stiffness which is reflected by the specific stiffness value, the only metal equivalent to the performance of aluminum is stainless steel. But the carbon fibre sheet outperforms the metals in both areas.

Table 1. Comparison of Mask Materials

Material	CTE, ppm/°C	Specific Stiffness*	Approx. Cost/Mask	Temp. Range**
Aluminum	23	2.6×10^6	$1	0.6 °C
Stainless Steel	9.5	2.7×10^6	$2	1.5°C
Niobium	7.1	1.1×10^3	$17	2.1°C
Zirconium	5.9	4.0×10^3	$10	2.5°C
Molybdenum	5.0	2.7×10^3	$27	2.9°C
Invar	1.0	1.8×10^6	$3	14.6°C
Graphite Paper	<0.1	N/A	$3	146°C
Carbon Fibre***	<0.1, along fibre ~15, across fibre	10×10^6, along fibre	$4	146°C

*Elastic modulus divided by weight density
** Allowable temp. variation not exceeding the ±3mm tolerance
*** Typical values for unidirectional laminate

3.2 Investigation of High Precision Cutting Processes

3.2.1 Photo-Chemical Etching

Photo-Chemical Etching is a multi-step process involving application of a photographic resist coating on the mask material, exposure and developing the coating to generate an etch pattern, then a final chemical etch to remove unwanted material and to produce the final slit pattern. This process uses photographic chemicals and strong acid or alkaline solution. The suppliers indicated that to develop a system meeting the level of precision and automation required would not be economical and pointed out the growing environmental concerns with the governmental regulatory agency over the usage of potentially hazardous chemicals at the telescope summit. Therefore, after internal discussion at the Dominion Astrophysical Observatory (DAO), it was decided not to pursue this as a mask making option.

3.2.2 Water-Jet Cutting

Water-jet cutting removes unwanted material by a fine jet of high pressure and high velocity water or water with abrasive particle additive. Therefore material can be removed at a high rate and without excessive heat dissipation regardless the hardness of the workpiece material.

Initially, three suppliers were contacted and each was sent a 100 µm thick stainless steel sample for cutting tests. But only one sample was returned while the other suppliers were reluctant to give any explanation for the cause of their tardiness. The slits on the sample received showed a kerf width of almost 1 mm which was cut by a 120 µm diameter nozzle. It seemed to indicate that in order to generate a 120 µm kerf, a nozzle of several times smaller would be required. However, small nozzle precluded the use of abrasive additive therefore cutting was achieved only after multiple passes at low feed rate for the 120 µm diameter nozzle. Therefore, it was concluded that water-jet cutting cannot be considered as a candidate mask making process in terms of cutting speed and precision.

3.2.3 Electric Discharge Machining (EDM)

EDM removes unwanted material by the erosive action of electric sparks between the cutter electrode and workpiece submerged in a dielectric fluid. The dielectric fluid insulates between the electrode and workpiece until sufficient voltage is applied to ensure effective electric erosion. Thus, EDM is limited to cutting electrically conductive materials.

For mask fabrication, a slit pattern can be produced by an electrode with thickness matching the required slit width. Theoretically, a linear cutting rate as high as 1.5 m per hour could be achieved while cutting through thin material, experienced EDM user indicated that the realized cutting rate for a complete slit pattern could take ten to fifteen times longer. After preliminary investigation, it was concluded that EDM lack the flexibility and speed to be considered an efficient mask making process.

3.2.4 Computer Numerical Control (CNC) Machining

During the investigation, it was learnt that engineers at the Lick Observatory had successfully cut 350 µm wide slits on their aluminum mask for the DEIMOS spectrograph by using a CNC milling machine with a high-speed spindle. Therefore, cutting trials using a 125µm diameter carbide cutter on a high-speed (~30,000 rpm) precision drill press were attempted at DAO. Two materials were tested, 120 µm Invar and 190 µm thick carbon fibre sheet. In the Invar trial, the cutter broke before it could cut through the material; and in the carbon fibre trial, the slit edge exhibited a number of whisker-like protrusions as seen in Figure 1. Since the drill press cutting test lacked the fine feed rate control of a CNC machine, the same thickness Invar sample was sent to Lick Observatory along with the 125 µm diameter carbide cutters. Several slits were cut, the raw slits exhibited rough edges as seen in Figure 2. However, the burrs along the slit edge can be removed mechanically after cutting for additional fabrication time.

Slit cutting using high-speed (450,000 rpm) dental drill was also investigated; however, dental burr with diameter as small as 125 µm is not available and slits cut in carbon fibre with larger burrs also produced the same whisker-like protrusions as seen previously.

Therefore, it was concluded that CNC machining would be an effective process for mask fabrication with metal but not with carbon fibre. It was considered as an backup process if nothing more effective could be found.

3.2.5 Light Amplification by Stimulated Emission of Radiation (Laser) Cutting

By converting electrical energy into light energy then into concentrated heat energy by focusing the light into a small spot on the workpiece surface, unwanted material is removed as it melts and/or vaporizes under the intense heat applied. Although different type of Laser systems exist, the neodymium-doped, yttrium aluminum garnet (Nd:YAG) laser is widely used in commercial laser machining system. It offers a good blend of ease of use and economical operation along with a reasonable degree of efficiency. In fact, most suppliers contacted recommended their Nd:YAG laser system for the slit cutting application.

At CFHT, a Nd:YAG laser with an output of 18 watts is incorperated in their LAMA mask cutting machine. Four samples were sent to CFHT for cutting test, they were: 120 µm thick Invar, 50 µm thick stainless steel, 200 µm thick graphite paper and 190 µm thick carbon fibre sheet. The Invar sample exhibited reasonably smooth slit edges after multiple slow feed rate passes. The edge quality is seen in Figure 3. The stainless steel sample exhibited rough slit edges and warping of material around the slit. The edge quality is seen in Figure 4. The graphite paper sample can be cut at high feed rate but it also exhibited some edge roughness. The edge quality is seen in Figure 5. The graphite paper has additional disadvantages for being soft and can be torn easily, which make handling difficult. The carbon fibre sample can also be cut at high feed rate and it exhibited the best edge quality as seen in Figure 6.

The edge quality of the slit was confirmed by straightness and smoothness measurements with the PDS microdensitometer at DAO. The edge straightness and smoothness achieved in carbon fibre were within the 1.2 µm requirement. Moreover, the total time to fabricate a 200 slit mask with carbon fibre sheet is estimated to be about one hour, which is based on the measured time to cut a 120 µm by 3 mm slit in two passes of four seconds.

3.3 Summary of Mask Making system

After the investigation, 190 µm thick unidirectional carbon fibre sheet was the only material that meets the mask material requirements. It has the highest specific stiffness and the lowest CTE of the materials considered. It was also tested to have zero transmittance from 360 nm to 2500 nm and having a reflectance of 4.5% at 400 nm and rising monotonically to 5.5% at 2300 nm.

Carbon fibre cut by laser was the only mask making process that met the slit geometry and mask fabrication requirements. Turn-key Nd:YAG laser machining systems with precision motion stage meeting the slit-to-slit position accuracy requirements (after error minimization as described in Section 5) are commercially available from at least two vendors in North America. Alternatively, the laser cutting system including laser head and control module, and the high precision X-Y stage including motor drive, encoder and motion control module can be purchased separately and integrated readily at DAO.

4. Proposed Mask Handling System

The carbon fibre mask is attached to a mask frame which provides a rigid mounting structure for handling. The mask is fastened to the frame by magnets. Magnetic strips are glued along the parameter of the frame opening where the carbon fibre mask is inserted and removeable magnetic strips are placed on top of the mask thus effectively "clamping" the mask in between. Features are machined into the frame to allow for handling - fixturing at the laser machining system, manipulation within GMOS and positioning at the focal plane.

For GMOS, the mask frame must share the same handling system as the integral field unit (IFU). (The IFU is used to reformat a two-dimensional field of view into two long slits via a series of microlenses and fibre optic cables.) The handling system must be able to deliver and position the mask and IFU at the focal plane with a repeatability of 25 µm.

The proposed GMOS mask handling system is shown in Figure 7. The system stores slit masks and IFU's in a mask cassette when they are not in use at the focal plane. The mask cassette is mounted on the mask cassette stage which translates in the direction of the optical axis. This allows mask and IFU selection for transport to the focal plane. Four different configurations of cassettes are available that store various numbers of masks and IFUs. The configuration with no IFUs stores 24 masks. A mask release mechanism unlocks the mask or IFU from the cassette for transportation to the focal plane. A barcode reader is used to read each mask as it is removed from the cassette to automate the task of mask identification and data archiving.

The slit masks and IFUs are transported to the focal plane via a V roller track and the mask extractor stage. The extractor stage connects to the mask using the extractor grip mechanism. The grip uses a 3 turn type attachment to the mask frame and IFU.

At the focal plane, the mask frame is supported by a kinematic mount. The mount defines the position of the mask frame vertically with two hard defining V rollers and four spring loaded V rollers. A hard stop and a spring tension mechanism built into the grip mechanism define the mask frame position horizontally. This mount provides mask stability that meets the functional requirements. The focal plane support accommodates masks and IFUs in the same mount.

5. Minimizing Fabrication Errors

The major source of fabrication error is expected from the precision X-Y stage. Straightness of travel, flatness of travel, X-Y orthogonality and AbbJ error are some of the factors effecting the accuracy of the X-Y stage thus the slit position. Furthermore, the stage error can be separated into systematic and random errors. The systematic error is repeatable and therefore can be minimized by calibration; whereas the random error is inherent and non-repeatable.

The X-Y stage systematic error is calibrated by performing a mask to detector mapping. A matrix pinhole mask is produced by the mask making system and placed at the focal plane of the spectrograph. The pinholes are then imaged on the detector. The actual positions of pinhole measured at the detector are checked against their theoretical X-Y stage positions as commanded by the mask making system. The discrepancies form a fitting surface which is the transformation between the actual position on the detector and the corresponding X-Y stage position required.

Since the baseline mask making procedure for slit placement uses direct images taken from the GMOS detector, this technique will ensure slits to science objects alignment up to the limit of the random error of the X-Y stage. The repeatability of the stage is expected to be in the order of 1 µm.

6. Acknowledgement

The authors wish to thank the staff of the Canada-France-Hawaii Telescope and the Lick Observatory for their help on slit cutting, and the Gemini 8-M Telescopes Project. The Gemini 8-M Telescopes Project is managed by the Association of Universities for Research in Astronomy, for the National Science Foundation and the Gemini Board, under an international partnership agreement.

7. References

1. T.J. Davidge, R. Murowinski and J. Allington-Smith, "GMOS Functional Requirement", March 1996.

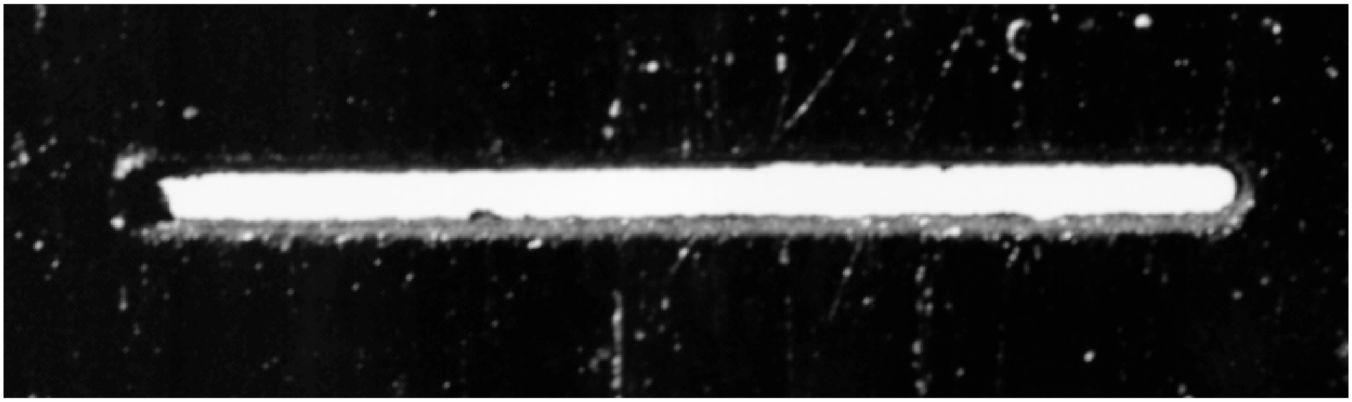

Figure 1. Milled Cut - 125µm wide slit in 190µm thick Carbon Fibre.

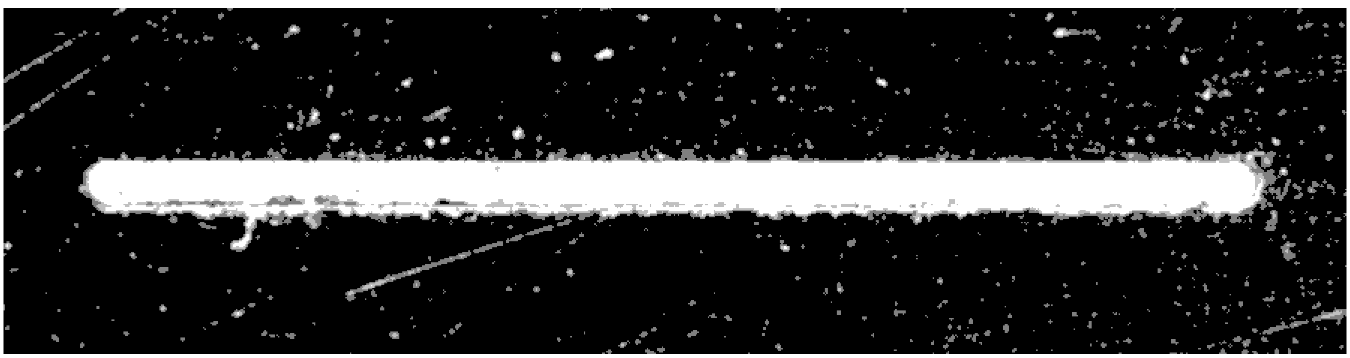

Figure 2. Milled Cut - 125µm wide slit in 190µm thick Invar.

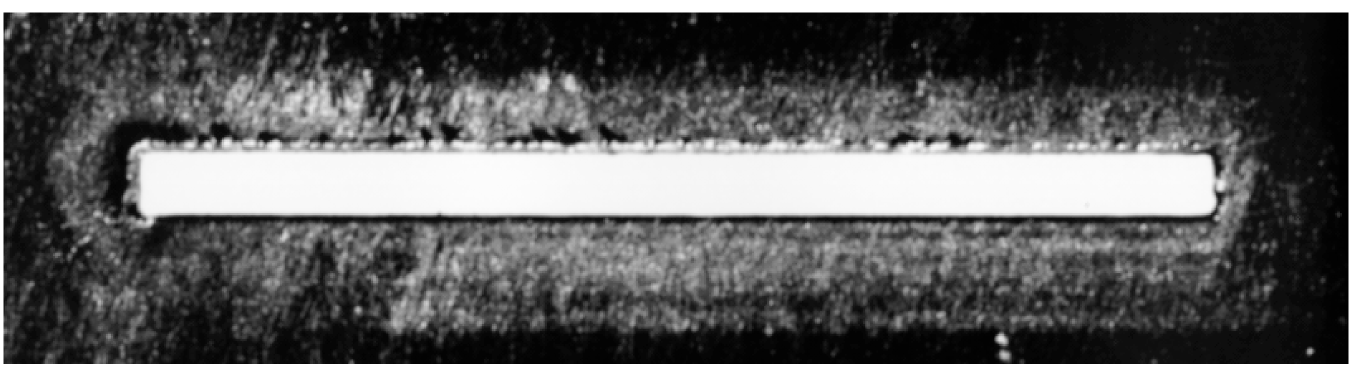

Figure 3. Laser Cut - 125µm wide slit in 190µm thick Stainless Steel.

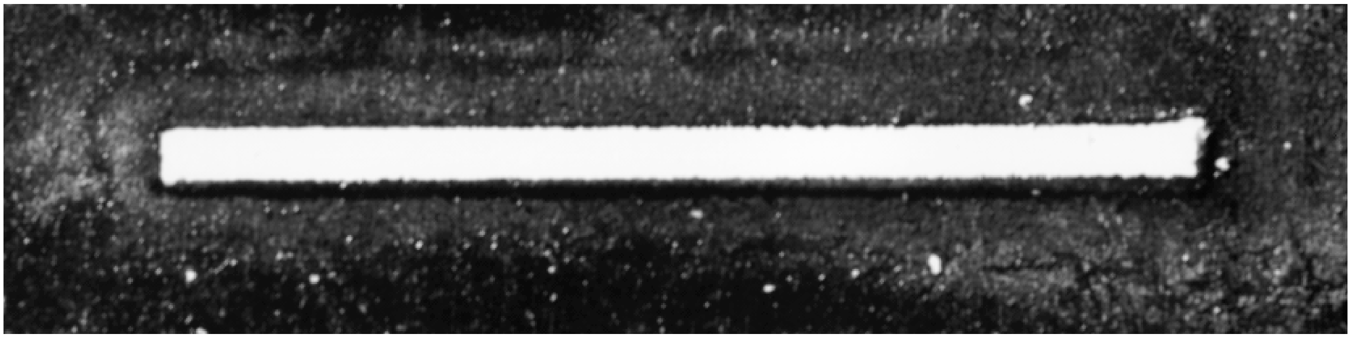

Figure 4. Laser Cut - 125µm wide slit in 50µm thick Stainless Steel.

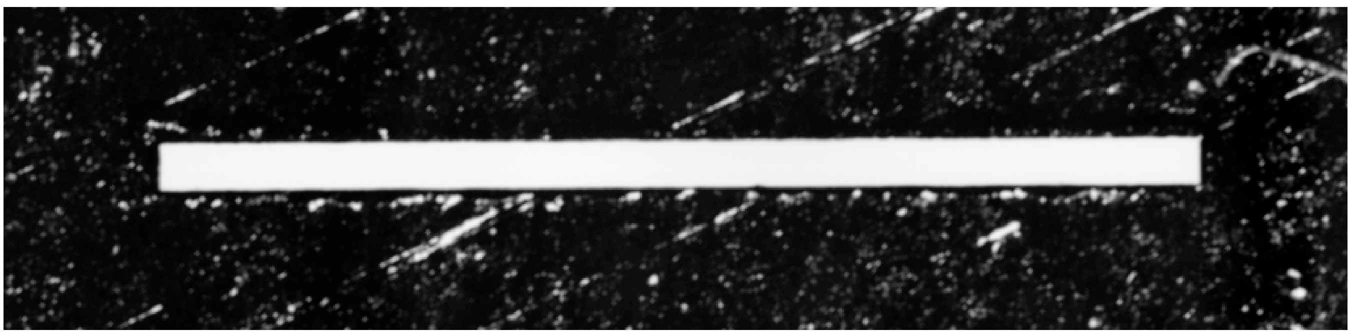

Figure 5. Laser Cut - 125µm wide slit in 190µm thick Graphite Paper.

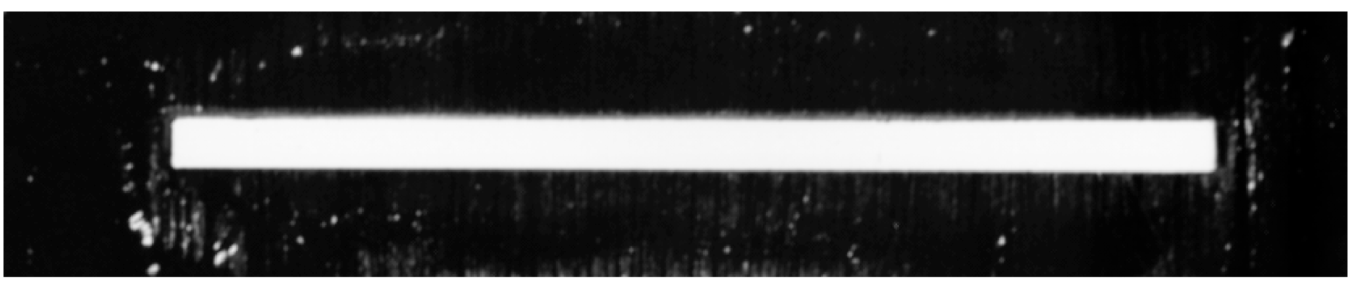

Figure 6. Laser Cut - 125µm wide slit in 190µm thick Carbon Fibre.

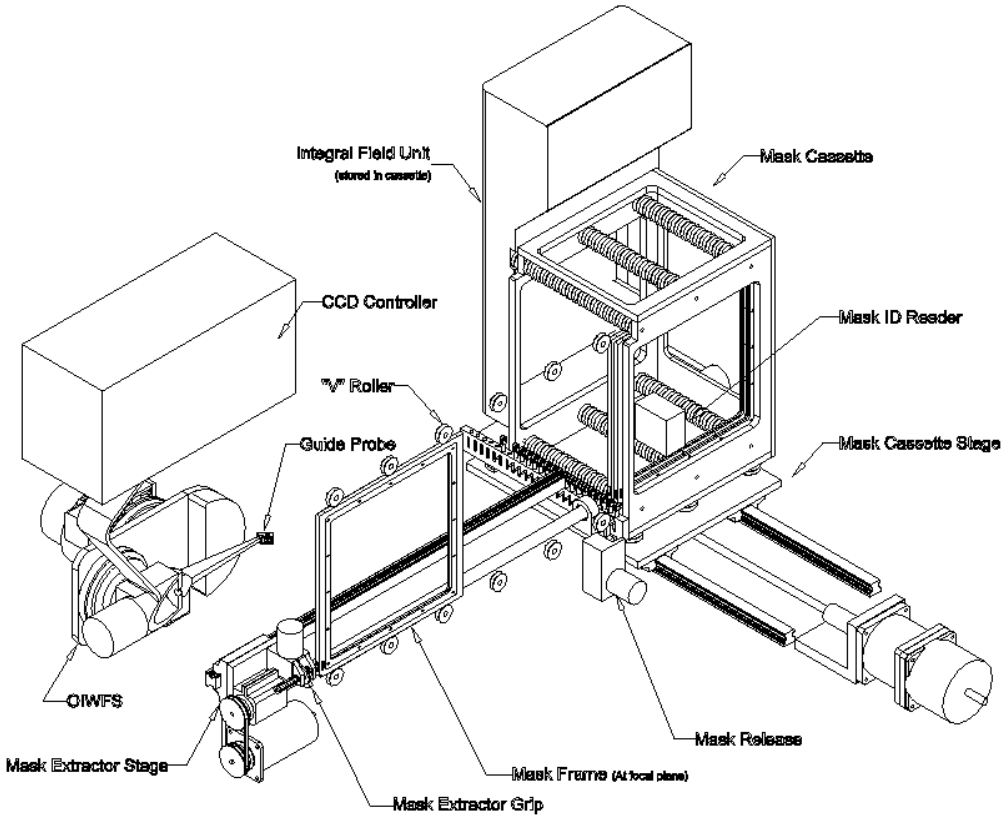

Figure 7. GMOS Mask Handling System.